Observation of Spin Seebeck Effect in Bulk Strontium Ferrite

Champ Suksawat* Poramed Wongjom** Dr.Supree Pinitsoontorn***

ABSTRACT

Spin Seebeck effect (SSE) can be observed in magnetized ferromagnetic materials when subjected to a temperature gradient.In this work, the results on the SSE in the bulk strontium ferrite were demonstrated for the first time. The SSE measurement was developed in our lab and calibrated with a $Y_3Fe_5O_{12}$ standard sample. The bulk strontium ferrite was characterized for the crystal structure and magnetic properties. It was then cut, ground and polished, before the Pt film was deposited on the surface. When subjected to the magnetic field and temperature gradient, the strontium ferrite showed the SSE signal which could be measured via the inversed spin Hall effect (ISHE). The SSE voltages measured across the Pt film showed the dependence on the magnetic field, the temperature gradient, and the Pt thickness, with the maximum signal of about 200 nV/K.

Keywords: Spin seebeck effect, Inveraed spin hall effect

* *Student, Master of Science Program in Physics, Department of Physics,Faculty of Science, Khon Kaen University*

** *Student, Doctor of Philosophy Program in Physics, Department of Physics,Faculty of Science, Khon Kaen University*

*** *Associate Professor, Department of Physics, Faculty of Science, Khon Kaen University*

Introduction

Spin caloritronics is devoted to the study of thermoelectric transport effects in materials systems where non-equillibrium spin populations occur. Recently, there have been a number of exciting discoveries in this research field(Johnson 2010). This includes the thermally driven spin injection from a ferromagnet into a non-magnetic metal(Slachter et al. 2010), Seebeck effect in magnetic tunnel junctions(Walter et al. 2011), and thermal spin current from a ferromagnet to silicon by Seebeck spin tunneling(Le Breton et al. 2011). All of these phenomena stimulate the potential to create and manipulate spin using heat. However, the most intriguing research in the field is the discovery of the spin Seebeck effect (SSE), which was first observed by Uchida and his co-workers (Uchida et al. 2008). In their experimental setups, temperature gradient was applied to a magnetized ferromagnetic material (NiFe film), and the spin accumulations were observed in the opposite ends of the sample. This effect requires magnetic field to create spin-polarization; thus it can be distinguished from a conventional Seebeck effect (Figure 1). Moreover, the direction of the magnetization is parallel to the temperature gradient; the SSE is, hence, dissociated from theNernst effect(Rowe 2006). The SSE was observed over a long distance (mm) which is much greater than the spin diffusion length(Bass and Pratt 2007). Although the theory behind the SSE was not clear, this discovery has opened up the applicability to produce spin-voltage generators, which are crucial for driving spintronic devices.

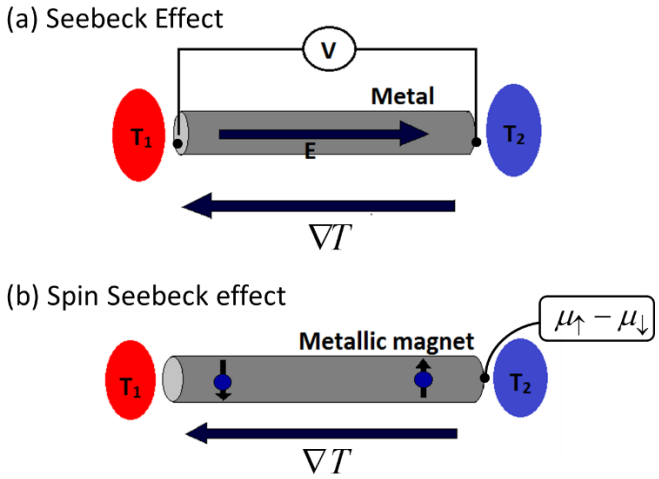

Figure 1 Illustration of **(a)** Seebeck effect and **(b)** spin Seebeck effect (SSE). In **(a)** Seebeck effect, a metal is subjected to a temperature gradient, and the electrical voltage difference is generated at both ends of the metal. In **(b)** SSE, a metallic magnet is subjected to a temperature gradient. Spin-up and spin-down electrons scatter at different rate resulting in the difference in spin accumulation at both ends of the magnet. The spin accumulation can be detected by inversed spin Hall effect (ISHE).

When the SSE was discovered (Uchida et al. 2008), the spin accumulation was detected by using a recently developed inversed spin Hall effect (ISHE)(Saitoh et al. 2006, Seki et al. 2008). The Pt stripe was deposited to both ends of the NiFe film. The ISHE converted a spin current into an electromotive force E_{SHE} by means of spin-orbit

scattering (which is enhanced in noble metals such as Pt). The E_{SHE} is related to a spin-polarization vector ($\vec{\sigma}$), and the spin current spatial direction ($\vec{J}_S$) by

$$\vec{E}_{SHE} = D_{ISHE}\vec{J}_S \times \vec{\sigma} \quad (1)$$

where D_{ISHE} is a coefficient representing the ISHE efficiency in a material. Uchida et al. has extended their works to observe the SSE in other metallic films such as Ni and Fe(Uchida et al. 2010). They have also studied the effect of Pt wire position and length(Uchida et al. 2009), the dependence on magnetic field and the temperature difference(Uchida et al. 2008, Uchida et al. 2010, Uchida et al. 2010). The results showed that the SSE is real. The E_{SHE} signal depends on the spatial distribution and the length of the Pt wire. It is also linearly proportional to the temperature difference between the hot and cold ends. The magnetic angle variation experiment has proved that the E_{SHE} varies sinusoidally according to equation (1).

Apart from conductive metallic magnets, the SSE wasobserved in the ferromagnetic semiconductor ($Ga_{1-x}Mn_xAs$) thin films grown on semi-insulating GaAs substrate(Jaworski et al. 2010), and in the magnetic insulator $LaY_2Fe_5O_{12}$, where conduction electrons are absent(Uchida et al. 2010). Furthermore, the SSE was observed not only in thin film but also in bulk materials. Bulk single crystal magnetic insulator $Y_3Fe_5O_{12}$(Uchida et al. 2010) as well as sintered polycrystalline $(Mn,Zn)Fe_2O_4$(Uchida et al. 2010) showed the SSE signal of the same order of magnitude as the ferromagnetic films. Subsequently, a variety of garnet ferrites ($Y_{3-x}R_xFe_{5-y}M_yO_{12}$, R= Gd, Ca; M = Al, Mn, V, In, Zr) were explored for the generation of the SSE signals (Uchida et al. 2013). It was found that the SSE signal was enhanced with increasing concentration of Fe in the garnet ferrites, and the SSE signal has a positive correlation with the Curie temperature and the saturation magnetization.

In this work, we present the study of the SSE in bulk strontium ferrite. The SSE measurement apparatus was developed and calibrated with the standard sample. As far as we are concerned, the SSE in this kind of ferrite has not been investigated before. The variable parameters in this study are the magnetic field, Pt film thickness, temperature gradient, and measurement temperature.

Objective of the study

To investigate the spin Seebeck effect in bulk strontium ferrite as a function of magnetic field, Pt film thickness, temperature gradient, and measurement temperature.

Materials and Methods

Sample preparation and characterization

A strontium ferrite magnet was purchased from a commercial available source and used without further modification. The sample was characterized for the phase and crystal structure using the X-ray diffraction (XRD) with K-α radiation (PANalytical, Empyrean, USA). The chemical compositionwas analyzed using the energy dispersive X-ray spectroscopy (EDS: Oxford, UK) equipped in the scanning electron microscope (SEM: LEO, 1450VP, UK). The magnetic property of the sample was investigated using the vibrating sample magnetometer

(VSM: Quantum Design, VersaLab, USA) at the maximum magnetic field of 30 kOe. The measurement was performed at 300 K and at 50 K.

For SSE measurement, the sample was cut into the dimension of 2 mm wide × 6 mm long × 1 mm thick using a slow-saw diamond blade (Fig. 2a). After thatthe sample was ground using sandpaper with 1,200 mesh and 2,000 mesh, respectively, to obtain very flat and smooth surface. Finally, it was polished with alumina paste (particle size < 1.0 μm) until metallic shiny surface was observed (Fig. 2b). Platinum film was deposited on the shiny surface of the strontium ferrite using the DC plasma sputtering technique (Fig. 2c).The sputtering current was fixed at 15 mA but the sputtering time was varied: 3.5, 4.5 and 6.0 minutes. The Pt film thickness was measured using the cross-section SEM images.Gold wire leads were connected to the opposite ends of the Pt surface along the length of the sample for voltage measurement in the SSE experiments. Small amount of Ag paste was used for gluing gold wires.

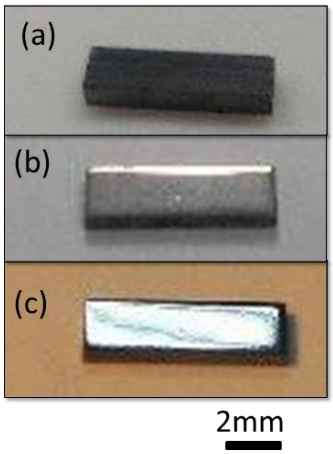

Figure 2 Sample preparation of strontium ferrite **(a)** after diamond blade cutting into the size of 2 mm × 6 mm × 1 mm, **(b)** after grinding and polishing, **(c)** after Pt film sputtered deposition

Spin Seebeck effect measurement set up

The SSE measurement apparatus was developed in our lab. The system was firstly designed and constructed as shown in Fig. 3. It consisted of a Cu block for heat dissipation (heat sink), a heater for applying temperature gradient to the sample, and the thermocouples for monitoring the temperature differences. The heater could supply the temperature difference up to 20 °C. The sample was loaded in the system as shown in Figure 3. To avoid the electrical short circuit, the sample was sandwiched between the insulating plates, separating it from the Cu block. The electrical insulator is made of AlN which has high thermal conductivity (>100 $W.m^{-1}K^{-1}$) for good thermal contact. The whole system was inserted into the chamber of the VersaLab (Quantum Design, USA). The magnetic field up to 30 kOe was applied, and the SSE measurement was carried out at the temperature ranging from 50 to 300 K. The schematic diagram of the direction of the temperature gradient and the magnetic field is shown in Figure 3d. The temperature gradient was applied in z direction whereas the magnetic field is applied along the x direction. This made the spin current ($\vec{J}_S$) injected from the ferrite to the Pt film in the z direction. Since the spin-polarization vector ($\vec{\sigma}$)

was in the same direction as the magnetic field (x axis), according to Equation (1), this produced the E_{SHE} in y direction across the length of the sample. The voltage then could be measured via the gold wire contacts. Due to a relatively low signal and to minimize noises, the voltage was detected using a nanovoltmeter (Keithely 2182A, USA). To test the in-house built SSE measurement system, we used the standard ($Y_3Fe_5O_{12}$) YIG thin film, received from Institute for Materials Research, Tohoku University, Japan, for measuring the SSE signal. Once the system is calibrated, the SSE experiment on the strontium ferrite was then carried out.

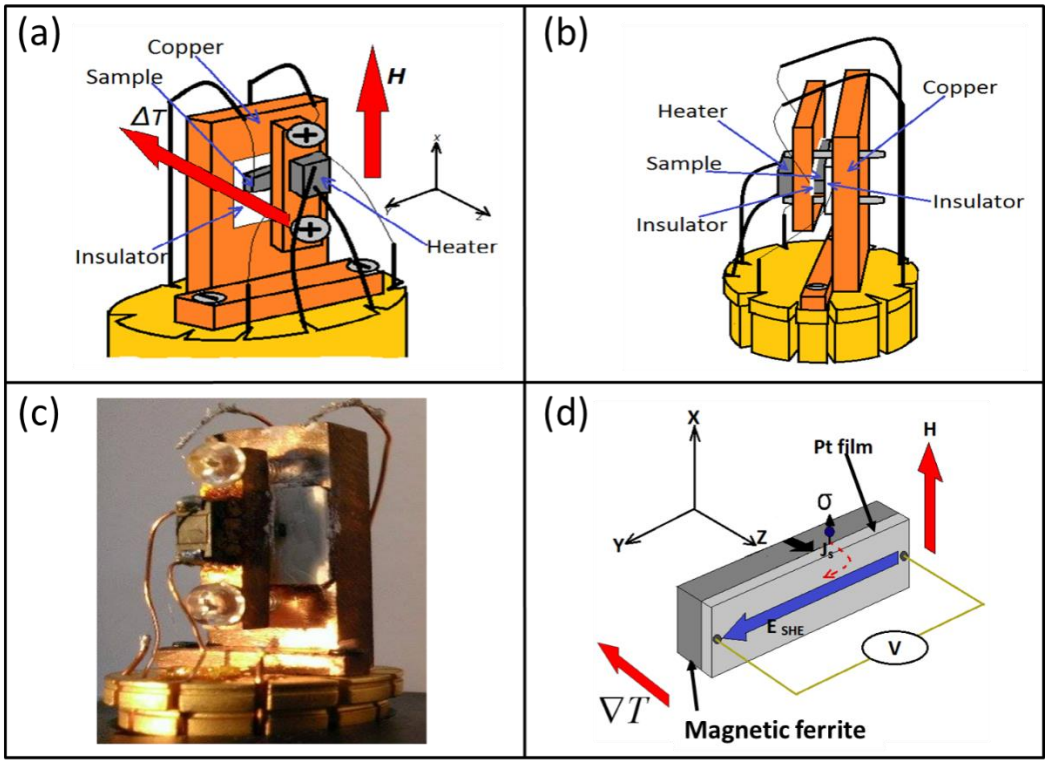

Figure 3 Experimental set up for SSE measurement: **(a)**and **(b)**the design of the in-house built apparatus consisting of Cu block, heater, thermocouple and insulator, **(c)** the image of the real apparatus. **(d)** the schematic diagram of the orientation of the sample, temperature gradient ad magnetic field direction. The spin current ($\vec{J}_S$) and a spin-polarization ($\vec{\sigma}$) generated the electromotive force E_{SHE} in y direction according to Equation (1).

Results

The XRD pattern of the bulk strontium ferrite is shown in Figure 4 alongside with the reference patterns. The miller indices were labelled in the pattern showing the strongest diffracted peaks at (220) plane. By comparing with the references, it is clearly seen that the sample has a combined phases between the $FeO_{2.558}Sr$ (ICDD 01-075-2827) and the $Fe_{2.937}O_4$(ICDD 01-086-1350). The carbon peaks (ICDD 00-050-0926) can also be seen, but probably due to the artefacts from processing.

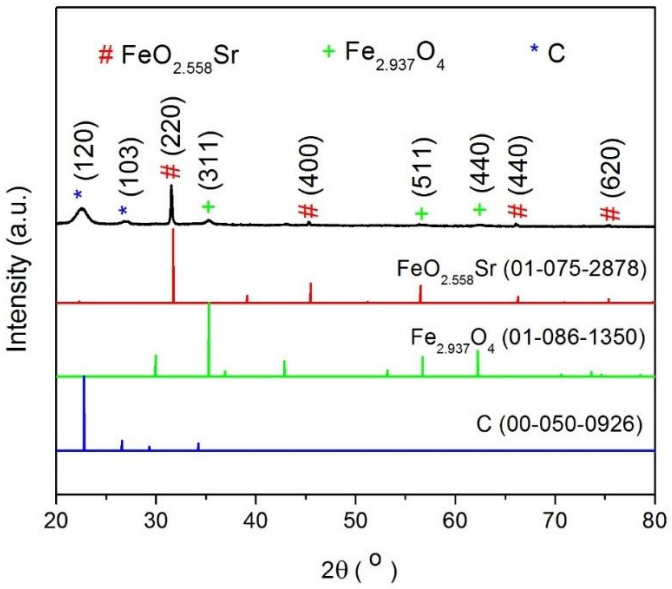

Figure 4 XRD pattern of the strontium ferrite alongside with the reference patterns,

The chemical composition of the sample was analyzed by using EDS technique, as shown in Figure 5. It is clearly observed that the spectrum consists mostly of the Fe K&L-edge peaks, the Sr L-edge peak, and the O K-edge peak. The composition by weight% and atomic% is summarized in the table in Figure 5.

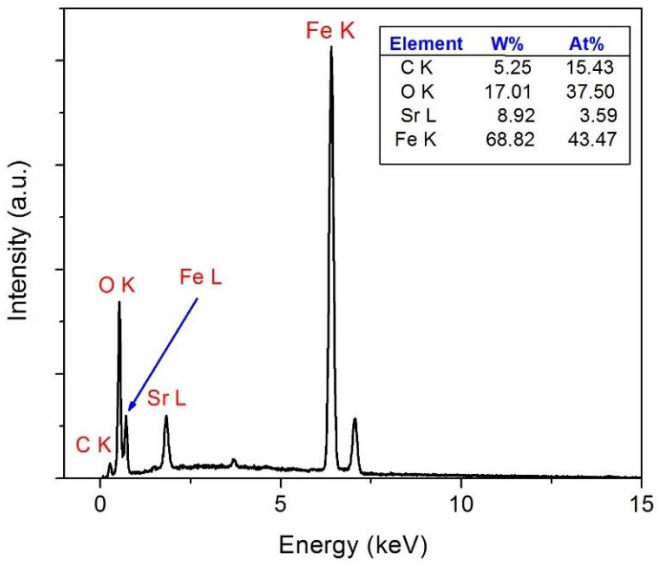

Figure 5 EDS spectrum of the strontium ferrite and the chemical composition analysis

The magnetization curves of the strontium ferrite sample measured at 300 K and 50 K is shown in Figure 6. The magnetic hysteresis loops were obtained at both 300 K and 50 K representing the ferromagnetic characteristics but the magnetization at 50 K is much stronger with the saturation magnetization around95 emu/g. At 50 K the loop

width is also larger due to the lower thermal fluctuation at lower temperature. Nevertheless, at both temperature the magnetizations are saturated at the magnetic field above 20 kOe.

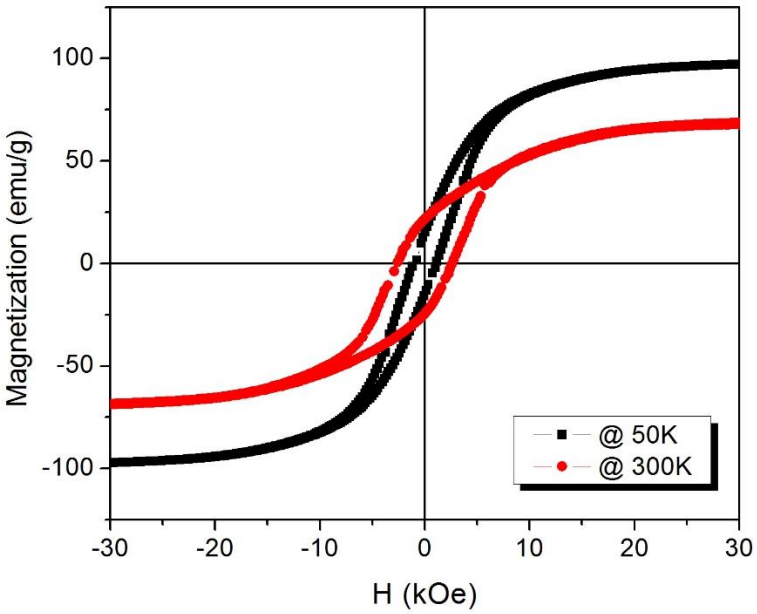

Figure 6 Magnetization hysteresis loop of the strontium ferrite measured at 300 and 50 K.

The polished surface of the strontium ferrite was coated with Pt film by sputtering deposition for the SSE measurement. The thickness of the film is related to the sputtering time as shown in the cross-section SEM images in Figure 7. The Pt films are roughly 1, 2 and 9 μm thick for the deposition time of 3.5, 4.5, and 6.0 minutes, respectively.

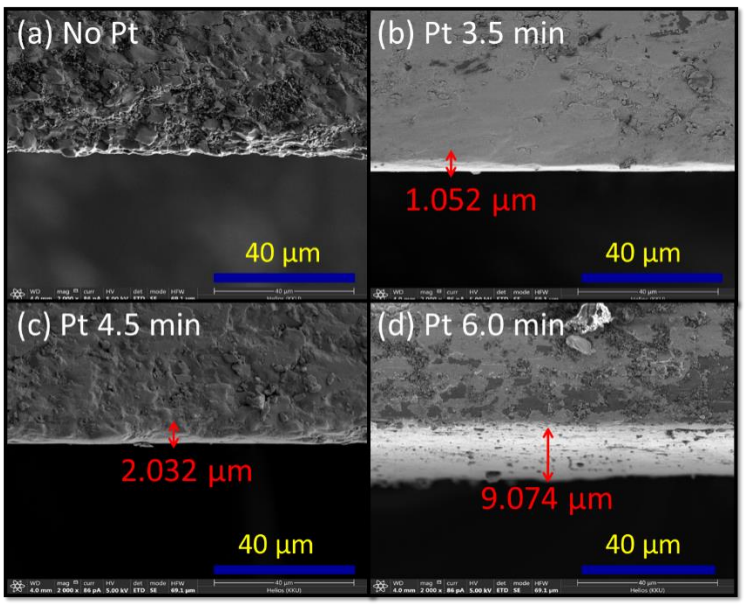

Figure 7 SEM Cross-section images of the strontium ferrite **(a)** without Pt film, and **(b)-(d)** with Pt film.

For the SSE measurement, we firstly present the result of the YIG standard sample (Figure8). The measured voltage was plotted against the applied magnetic field from -3,000 to 3,000 Oe. It is clearly seen that without applying the temperature gradient the SSE voltage is nearly zero for the whole range of the magnetic field (black curve). When the temperature difference of 6 °Cwas applied to the sample, the SSE voltage was induced (red curve). The signal is non-linearly proportional to the magnetic field. In fact, the SSE voltage dependence of H has a shape similar to the magnetic hysteresis loop. The SSE voltage is saturated at nearly 4 μV at the field above 1,000 Oe. The characteristics and the saturation value of the SSE in YIG observed in our experiment is similar to previously published research (Uchida et al. 2010, Uchida et al. 2010, Uchida et al. 2013). It is concluded that our apparatus shows a reliable result for SSE measurement and thus can be used for measuring the SSE in bulk strontium ferrite.

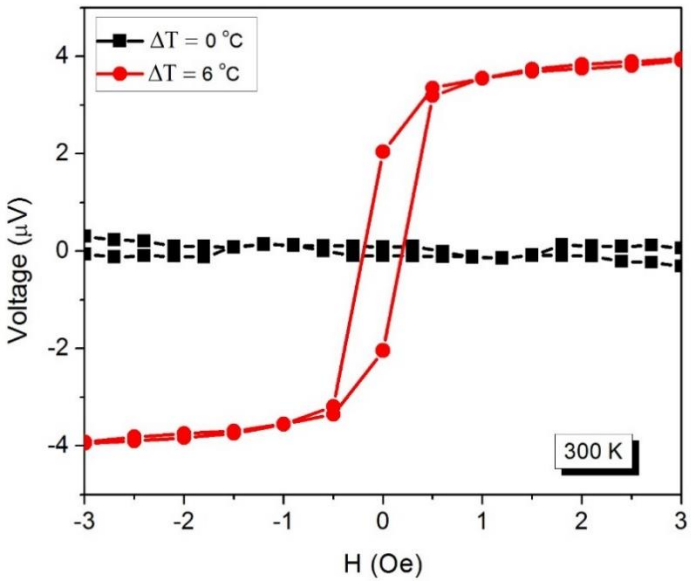

Figure 8 SSE measurement of Pt/YIG thin film showing the SSE voltage only when the temperature gradient is applied.

The SSE measurements in strontium ferrite as a function of magnetic field and temperature difference are presented in Figure 9. The points are the collected data and the straight lines are the linear fits of the data. For the measurement at 300 K (Figure 8a), without applying temperature gradient, the SSE voltage has a negative slope with the applying magnetic field. When applying the temperature gradient, the slope becomes positive and the value is larger as the temperature difference is higher. A similar trend is found for the measurement at 50 K but the magnitude of the SSE signal is larger due to the thermal noise is more suppressed at lower measurement temperature. The experiment in this part shows the existence of the SSE in the bulk strontium ferrite. The SSE signal could be observed only if the temperature gradient and the magnetic field are present simultaneously as predicted by theories. Without either one, the voltage could not be detected. All data in this section was collected with the Pt film deposited for 6.0 minutes.

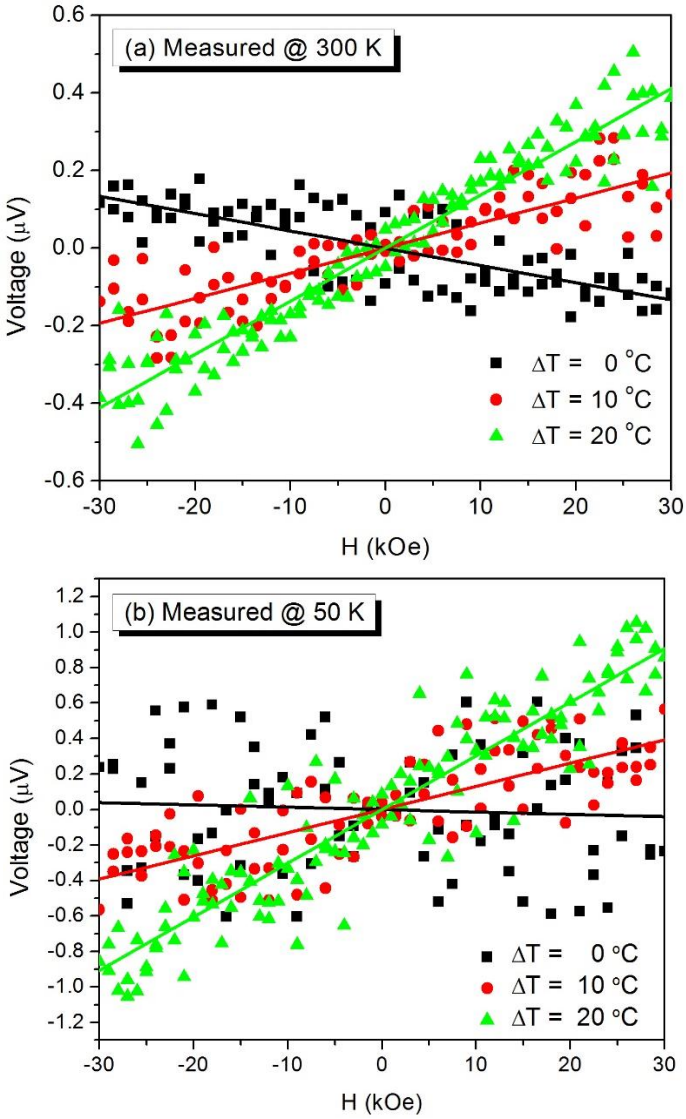

Figure 9 SSE of Pt/ferriteas a function of magnetic fields and temperature differences, measured at (a) 300 K and (b) 50 K. All data was collected with the Pt film deposited for 6.0 min.

Figure 10 shows the SSE voltage of Pt/ferrite as a function of the magnetic field and the Pt film thickness. In the presence of the magnetic field, the SSE signals increase with Pt thickness. At 300 K (Figure 10a), for the magnetic field of 30 kOe, the SSE voltage is approximately 0.4 μV for the ferrite with 6.0-min Pt film but the signal is only 0.1 μV for the sample with 3.5-min Pt deposition. The reason could be due to the higher electrical conductivity of the thicker Pt film. The resistances of the Pt films were 982 □,252 □,157 □ for Pt deposition of 3.5, 4.5 and 6.0 min, respectively. Again, the same trend was found but the signals were stronger for the experiment at 50 K. All data in this section was collected at the temperature difference of 20°C

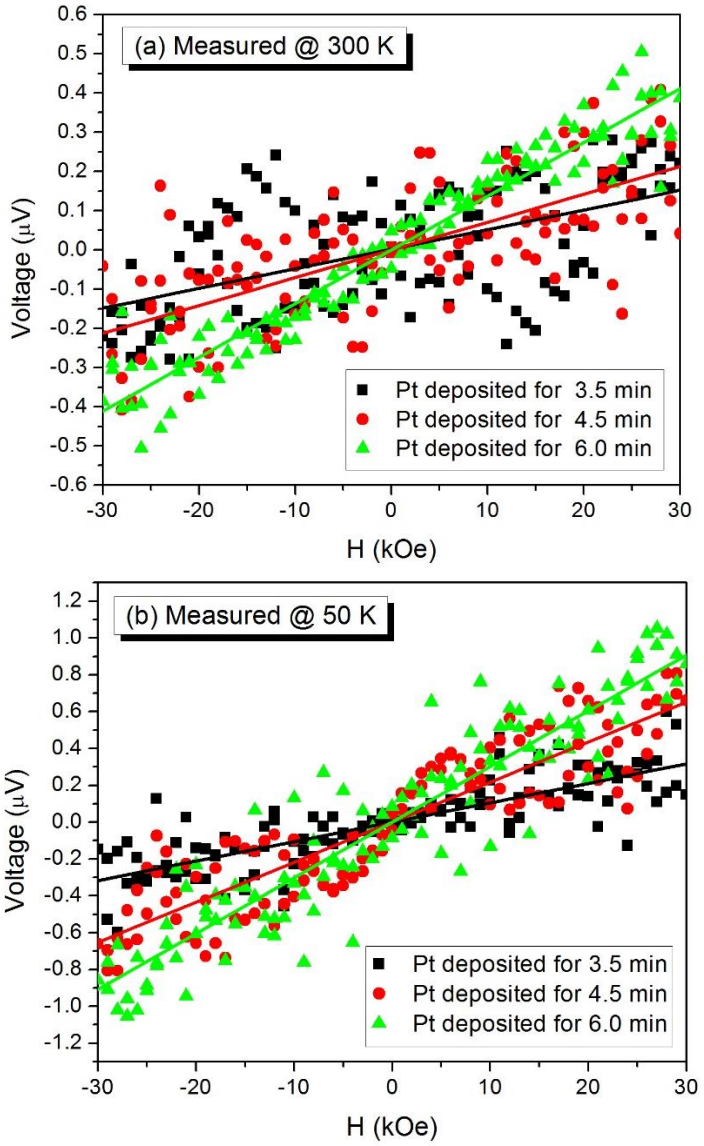

Figure 10 SSE of Pt/ferrite as a function of magnetic fields and Pt film thickness, measured at (a) 300 K and (b) 50 K. All data was collected with the temperature difference of 20°C.

Discussion

This work has demonstrated that the SSE can be observed in the bulk strontium ferrite by using our in-house built apparatus. Since the sample is highly electrical insulated, the observed SSE in our experiment is thus believed to be a result of the phonon-magnon coupling as suggested by a recently developed theory(Adachi et al. 2011, Jaworski et al. 2011, Uchida et al. 2011). However, there are a few differences between our work and the SSE in other magnetic insulator systems (Uchida et al. 2010, Uchida et al. 2010, Uchida et al. 2010, Uchida et al. 2013). Firstly, our SSE signal in the strontium ferrite is linearly dependent on the magnetic field. No sign of saturation, like in magnetic hysteresis loop, is observed. Secondly, the magnitude of the voltage per ΔT in our experiment is much lower than the previous reports. Our spin Seebeck voltage (V_{ss}) per ΔT is about 0.02 μV/K or 200 nV/K but $V_{ss}/\Delta T$

were reported to be approximately 0.2 μV/K and 0.5 μV/K for the sintered polycrystalline (Mn,Zn)Fe_2O_4 and the YIG slap, respectively (Uchida et al. 2010, Uchida et al. 2010). The value of the present experiment is one order of magnitude lower than literatures. The discrepancies between our SSE observation and previous reports are likely to be from the surface roughness of the strontium ferrite. As can be seen in Figure 7, the roughness of the uncoated sample is obviously observed. This would cause significant deterioration of spin injection from the ferrite to the Pt film. In further works, the smoothness of the ferrite surface needs significant improvement. In addition, the Pt thickness needs optimization for obtaining the maximum SSE signal.

Conclusions

We have demonstrated the SSE in the bulk strontium ferrite for the first time. The SSE signal is real and can be distinguished from the ordinary Seebeck effect since it could be observed only when the magnetic field and temperature gradient were applied simultaneously. It can also be excluded from the Nerst effect because of the different orientation set up. The SSE voltage measured across the Pt film increased with the magnetic field, the temperature gradient and the Pt thickness, with the maximum signal of about 200 nV/K. However, there are several works to be done in the future, including improving the surface smoothness of the strontium ferrite and optimizing the Pt film thickness.

Acknowledgements

This study was supported by the Thailand Research Fund (TRF) in cooperation with Khon Kaen University (RSA5980014), and the Integrated Nanotechnology Research Center, Khon Kaen University.We would like to thank Assoc. Prof. Ken-ichi Uchida and Dr. Rafael Ramos at Institute for Materials Research, Tohoku University, Japan,for providing us the standard YIG sample, and for their insightful suggestions.

References

Adachi H, Ohe J, Takahashi S, Maekawa S. Linear-response theory of spin Seebeck effect in ferromagnetic insulators. Phys Rev B 2011; 83(9): 094410.

Bass J, Pratt WP. Spin-diffusion lengths in metals and alloys, and spin-flipping at metal/metal interfaces: an experimentalist's critical review. J Phys-Condens Mat 2007; 19(18): 183201.

Jaworski CM, Yang J, Mack S, Awschalom DD, Heremans JP, Myers RC. Observation of the spin-Seebeck effect in a ferromagnetic semiconductor. Nat Mater 2010; 9(11): 898-903.

Jaworski CM, Yang J, Mack S, Awschalom DD, Myers RC, Heremans JP. Spin-Seebeck Effect: A Phonon Driven Spin Distribution. Phys Rev Lett 2011; 106(18): 186601.

Johnson M. Spin caloritronics and the thermomagnetoelectric system. Solid State Commun 2010; 150(11-12): 543-547.

Le Breton JC, Sharma S, Saito H, Yuasa S, Jansen R. Thermal spin current from a ferromagnet to silicon by Seebeck spin tunnelling. Nature 2011; 475(7354): 82-85.

Rowe DM. Thermoelectrics handbook : macro to nano. Boca Raton: CRC/Taylor & Francis; 2006.

Saitoh E, Ueda M, Miyajima H, Tatara G. Conversion of spin current into charge current at room temperature: Inverse spin-Hall effect. Appl Phys Lett 2006; 88(18): 182509.

Seki T, Hasegawa Y, Mitani S, Takahashi S, Imamura H, Maekawa S, et al. Giant spin Hall effect in perpendicularly spin-polarized FePt/Au devices. Nat Mater 2008; 7(2): 125-129.

Slachter A, Bakker FL, Adam JP, van Wees BJ. Thermally driven spin injection from a ferromagnet into a non-magnetic metal. Nat Phys 2010; 6(11): 879-882.

Uchida K, Adachi H, An T, Ota T, Toda M, Hillebrands B, et al. Long-range spin Seebeck effect and acoustic spin pumping. Nat Mater 2011; 10(10): 737-741.

Uchida K, Adachi H, Ota T, Nakayama H, Maekawa S, Saitoh E. Observation of longitudinal spin-Seebeck effect in magnetic insulators. Appl Phys Lett 2010; 97(17): 172505.

Uchida K, Nonaka T, Kikkawa T, Kajiwara Y, Saitoh E. Longitudinal spin Seebeck effect in various garnet ferrites. Phys Rev B 2013; 87(10): 104412.

Uchida K, Nonaka T, Ota T, Saitoh E. Longitudinal spin-Seebeck effect in sintered polycrystalline (Mn,Zn)Fe2O4. Appl Phys Lett 2010; 97(26): 262504.

Uchida K, Ota T, Harii K, Ando K, Nakayama H, Saitoh E. Electric detection of the spin-Seebeck effect in ferromagnetic metals (invited). J Appl Phys 2010; 107(9): 09A951.

Uchida K, Ota T, Harii K, Ando K, Sasage K, Nakayama H, et al. Spin Seebeck Effect in Ni81Fe19/Pt Thin Films With Different Widths. Ieee T Magn 2009; 45(6): 2386-2388.

Uchida K, Ota T, Harii K, Takahashi S, Maekawa S, Fujikawa Y, et al. Spin-Seebeck effects in Ni81Fe19/Pt films. Solid State Commun 2010; 150(11-12): 524-528.

Uchida K, Takahashi S, Harii K, Ieda J, Koshibae W, Ando K, et al. Observation of the spin Seebeck effect. Nature 2008; 455(7214): 778-781.

Uchida K, Xiao J, Adachi H, Ohe J, Takahashi S, Ieda J, et al. Spin Seebeck insulator. Nat Mater 2010; 9(11): 894-897.

Walter M, Walowski J, Zbarsky V, Munzenberg M, Schafers M, Ebke D, et al. Seebeck effect in magnetic tunnel junctions. Nat Mater 2011; 10(10): 742-746.